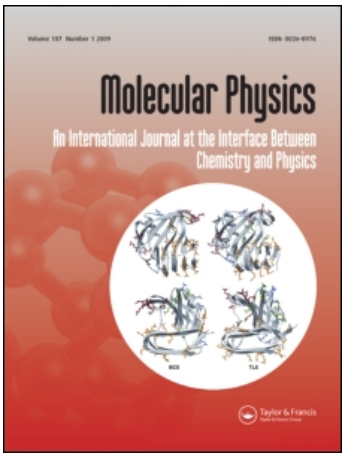

Molecular Physics
Publication details, including instructions for authors and subscription information:
http://www.informaworld.com/smpp/title~content=t713395160

Molecular dynamics simulation of the liquid mixture CCl_4/CS_2

U. Mittag [a]; J. Samios [a]; Th. Dorfmüller [a]
[a] Universität Bielefeld, Fakultät für Chemie, Physikalische Chemie I, Bielefeld 1, F.R. Germany

Online Publication Date: 01 January 1989

To cite this Article Mittag, U., Samios, J. and Dorfmüller, Th.(1989)'Molecular dynamics simulation of the liquid mixture CCl_4/CS_2',Molecular Physics,66:1,51 — 64
To link to this Article: DOI: 10.1080/00268978900100021
URL: http://dx.doi.org/10.1080/00268978900100021

MOLECULAR PHYSICS, 1989, VOL. 66, NO. 1, 51–64

Molecular dynamics simulation of the liquid mixture CCl_4/CS_2

I. Thermodynamic and structural properties

U. MITTAG, J. SAMIOS and TH. DORFMÜLLER
Universität Bielefeld, Fakultät für Chemie, Physikalische Chemie I, 4800 Bielefeld 1, F.R. Germany

(*Received 18 January 1988; accepted 19 August 1988*)

All centre–centre and atom–atom pair correlation functions have been calculated from a molecular dynamics simulation of the mixture CCl_4/CS_2 at three mole fractions and at room temperature. The agreement between the intermolecular correlation functions obtained and the corresponding data from a neutron scattering is excellent. The results are discussed in terms of the changes of the local environment of the CCl_4 and CS_2 molecules with changing mole fractions.

1. Introduction

It is well known that, due to differences of molecular sizes, shapes and interactions, the properties of liquid mixtures cannot be derived from those of pure substances. On the other hand, a deeper understanding of the thermodynamic and molecular behaviour of liquid mixtures in a wide temperature, composition, and pressure range is highly desirable not only from a theoretical point of view, but also for chemical engineering applications.

It has been shown that perturbation theory [1] was quite successful in describing binary liquid systems formed from non-polar spherical and nearly spherical molecules. However, the extension [2] of this theory to the case of systems containing two kinds of molecules varying widely in size and geometrical shape was not able satisfactorily to reproduce the experimental thermodynamic properties. The crucial points, in this particular case seem to be the following: how can the number and the position of interaction centres between like and unlike molecules be related to the correct geometrical molecular shapes; what is the form of the combining rules between interaction potentials of unlike molecules/atoms.

In recent years considerable advance has been made in computer simulation (CS) studies of the properties of molecular liquids. However, in the case of molecular liquid mixtures very little work has been done using CS techniques. To our knowledge only a few studies [3] using molecular dynamics (MD) have been carried out in mixtures. The present study represents a contribution to the study of the structure of the liquid mixture CCl_4/CS_2 by the MD method. The system was chosen for its 'simplicity' in the sense that its excess free energy and enthalpy are very small at room temperature (g^E, $h^E \ll RT$) and that the components display a perfect miscibility at all concentrations. Furthermore, both pure liquids have been extensively studied experimentally, theoretically, and by numerous MD simulations [4, 5]. In

0026–8976/89 $3.00

Table 1. Atom–atom L–J potential parameters for the liquid mixture CCl_4/CS_2.

	CCl_4–CCl_4†			CS_2–CS_2‡			CCl_4–CS_2		
Param.	C_A–C_A	Cl–Cl	C_A–Cl	C_B–C_B	S–S	C_B–S	C_A–C_B	C_A–S	Cl–C_B
E/k K	51·2	102·4	72·4	51·2	183·0	96·8	51·2	96·8	72·4
σ nm	0.460	0.35	0·405	0·335	0·352	0·344	0·398	0·406	0·434

† McDonald *et al.* in [4].
‡ Tildesley and Madden in [5].
C_A and C_B is the C atom in CCl_4 and CS_2 respectively.

addition, careful experimental measurements, of the thermodynamic properties at different temperatures and compositions [6], diffusion coefficients [7], and a large number of spectroscopic studies [8] have been published by several groups in the last decade.

In this paper we shall describe some MD calculations of the mixture at room temperature and three mole fractions ($x = 0{\cdot}25$, $x = 0{\cdot}5$ and $x = 0{\cdot}75$) with particular emphasis on the effective potential model, the total thermodynamic properties, and the atom–atom distribution functions. Most of these results are compared with corresponding experimental data.

2. Computational details

The theoretical understanding of intermolecular forces has improved in the last 15 years, especially in the case of very simple molecules by the application of perturbation theory and computer simulation methods. However, in the case of systems containing unlike and structured molecules, the problem of constructing an 'effective' potential which is capable of reproducing experimental features remains to be solved.

In a previous theoretical treatment, Bohn *et al.* [2] studied the adequacy of a proposed potential model for the mixture CCl_4/CS_2. The interaction between CCl_4–CCl_4 molecules was described by a one-centre 12–6 L–J potential, and those of the CS_2–CS_2 molecules by a two-centre 12–6 L–J potential. The calculated thermodynamic properties were not satisfactory, probably on account of the inadequacy of describing the interactions with only one and two centres. Finally, Coon *et al.* [9] performed isothermal–isobaric (NPT ensemble) MD simulation on the equimolar mixture CCl_4/CS_2 using the potential model of the previous theoretical work. The results were almost identical with those predicted theoretically but again very different from the experimental values. These attempts clearly show the necessity to construct a better model of the CCl_4/CS_2 mixture. Besides the necessity to better account for molecular shape by using more interaction centres the additional problem arises that no unambiguous prescription is available for modelling a potential between unlike atoms on the basis of the potentials of like atoms except for the Berthelot rules which are usually assumed to better approximate pure dispersion forces.

Previous successful MD studies of the pure liquids CCl_4 [4] and CS_2 [5] using atom–atom L–J potentials motivated us to adopt the same potential. Thus, the interaction between CCl_4–CCl_4 was described by a five-centre and those of CS_2–CS_2 by a three-centre 12–6 L–J potential. For the cross interaction terms the

Table 2. Technical features of the simulations of CCl_4/CS_2 liquid mixtures. The algorithm used was the quaternian predictor fifth order for the translation and fourth order for the rotation.

Conc. mol % CCl_4	No. of molec.	Temp/ K	Molar vol./ cm^3/mol	Time integ. step/ ps	Total time of simul- ations/ ps	Cutoff radius Å	Energy/(kJ/mol) Internal (sim)	Total (sim)	Internal (exp)†
0	108	298	60·38	0·005	90	11·06	25·3	19·05	25·42
25	500	298	69·83	0·005	160	11·61	26·9	20·43	26·91
50	500	298	79·08	0·005	145	12·10	28·6	21·81	28·51
75	500	298	88·22	0·005	130	12·55	30·3	23·29	30·26
100	108	298	97·15	0·005	95	12·96	32·2	24·55	32·21

† Calculated from the experimental heat of vaporization of the pure liquids and the excess enthalpies of mixing given in [6].

Lorentz–Berthelot mixing rules were used:

$$E_{ij} = [E_{ii} \cdot E_{jj}]^{1/2}, \tag{1 a}$$

$$\sigma_{ij} = [\sigma_{ii} + \sigma_{jj}]/2. \tag{1 b}$$

The values of the (12–6) L–J atom–atom potential parameters are shown in table 1.

The MD simulations were carried out in the microcanomical ensemble (N, V, E) by using 500 molecules in a cubic box with periodic boundary conditions. The bond lengths were: $d_{C-Cl} = 1{\cdot}77$ Å, $d_{Cl-Cl} = 2{\cdot}88$ Å and $d_{C-S} = 1{\cdot}57$ Å. All runs were initiated with the molecules arranged in an f.c.c. lattice. In the case of mixtures the molecules with the smaller concentration were located in free sites randomly created within the lattice. The most important computational data are tabulated in table 2. In order to distort the initial f.c.c. configuration to such a degree that a disordered liquid state configuration could be achieved within a short time the following procedure was used in each preliminary run: Each molecule was displaced by up to 10 per cent of the nearest-neighbour distance. Translational and rotational velocities were chosen randomly in direction and magnitude, so that the kinetic energy, both translational and rotational, corresponded to the classical equipartition value. The orientation of each molecule was also selected randomly. The equations of motion both translational and rotational were integrated by using an algorithm based on the quaternion method and adapted to a two-component system of linear and tetrahedral molecules. The relative energy drift was lower than 1 in 10^4 for the whole simulation. Equilibrium was achieved at ≈ 10 ps (for mixtures ≈ 40 ps) and the simulations were extended subsequently to ≈ 90 ps (for mixtures ≈ 140 ps). All molecular positions, orientations and velocities were stored on magnetic tape in intervals of 8 time steps over the total simulation time.

The derived mean potential energy U_{sim} (kJ/mol) and the corresponding experimental value U_{exp}(kJ/mol) are shown in table 2. As can be seen the agreement between U_{sim} and U_{exp} can be considered as quite satisfactory. The above result indicates that the used potential model can provide an acceptable prediction of the total internal energy which is very sensitive to this parameter. On the other hand, in liquid mixtures one is more interested in calculating excess properties rather than total properties. However this requires high precision calculations since such

properties are obtained as small differences between large numbers. In most cases the necessary precision cannot be achieved using conventional MD test-particle methods. The adequacy of the potential model for this kind of simulation was actually checked stepwise first on the basis of the calculated total thermodynamical properties and then by comparing our total intermolecular pair correlation function (IPCF) to neutron scattering results which have been obtained in a parallel collaborative study [10].

3. Intermolecular pair correlation functions

It is well known that a complete description of liquid structure requires the evaluation of all static atom–atom pair correlation functions (APCFs) $g_{\alpha\beta}(R)$, where R is the distance between atoms α and β belonging to two different molecules, and of molecular orientational correlation functions.

The APCFs can be experimentally determined by scattering experiments. Thus, X-ray, electron and neutron diffraction have been successfully used for this purpose [11]. Especially the latter method, if a convenient isotopic substitution is carried out, can be and has been successfully used in the past to obtain important structural data on pure liquids and liquid mixtures [12]. We briefly summarize the procedure by which the differential neutron scattering intensities can be analysed in order to study the structure of a binary liquid mixture of the species 'A' and 'B'.

The measured total neutron scattered intensity $(d\sigma/d\Omega)_{\text{tot}}$ can be split into a coherent and an incoherent contribution.

$$\left(\frac{d\sigma}{d\Omega}\right)_{\text{tot}} = \left(\frac{d\sigma}{d\Omega}\right)_{\text{inc}} + \left(\frac{d\sigma}{d\Omega}\right)_{\text{coh}}. \tag{2}$$

The former can be again split into a self and a distinct part

$$\left(\frac{d\sigma}{d\Omega}\right)_{\text{coh}} = \left(\frac{d\sigma}{d\Omega}\right)_{\text{coh}}^{\text{self}} + \left(\frac{d\sigma}{d\Omega}\right)_{\text{coh}}^{\text{dist}}. \tag{3}$$

Only the distinct coherent intensity contains information about the APCFs. Equation (4) represents the self coherent part, in the case of a N-component mixture with the mole fraction x_i

$$\left(\frac{d\sigma}{d\Omega}\right)_{\text{coh}}^{\text{self}} = \sum_{i=1}^{N} x_i \sum_{\alpha=1}^{n} b_{i\alpha}^2(\kappa). \tag{4}$$

The index i runs over the N components and the index α over the n atoms of the molecules of the ith component. The distinct coherent contribution is given by equation (5)

$$\left(\frac{d\sigma}{d\Omega}\right)_{\text{coh}}^{\text{dist}} = \rho \sum^{N} \sum^{N} x_{x_i x_j} \sum_{\alpha=1}^{n_i} \sum_{\beta=1}^{n_j} b_{i\alpha}(\kappa) b_{j\beta}(\kappa) h_{i\alpha j\beta}(\kappa). \tag{5}$$

The functions $h(\kappa)$ are the still unknown partial structure factors, ρ and x_i are the number density and the mole fraction respectively. As we can see from equation (5) the distinct coherent scattering contains intra- and intermolecular contributions

$$\left(\frac{d\sigma}{d\Omega}\right)_{\text{coh}}^{\text{dist}} = \left(\frac{d\sigma}{d\Omega}\right)_{\text{coh}}^{\text{dist, intra}} + \left(\frac{d\sigma}{d\Omega}\right)_{\text{coh}}^{\text{dist, int}}. \tag{6}$$

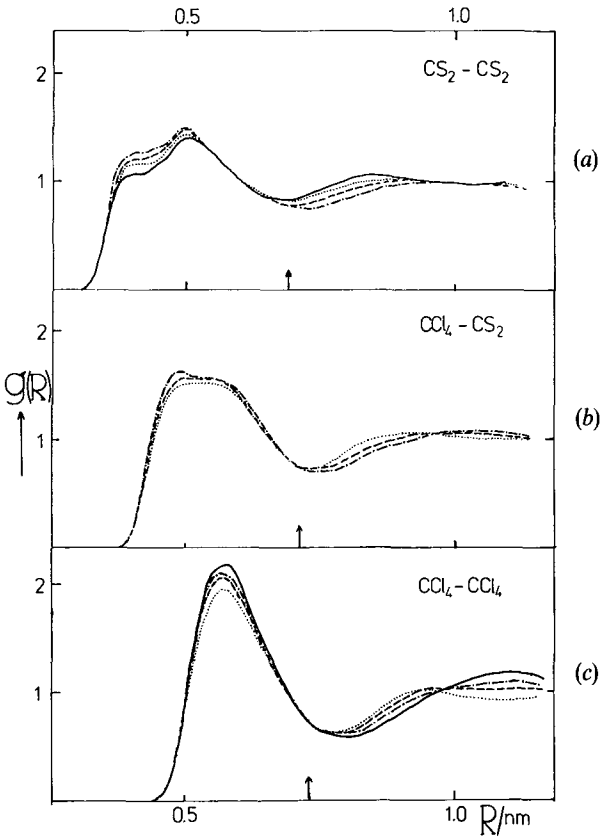

Figure 1. A plot of CS_2–CS_2 (C_B, C_B), CCl_4–CS_2 (C_A, C_B) and CCl_4–CCl_4 (C_A, C_A) centre–centre radial correlation functions (CCFs) obtained from this MD simulation study: ———, pure CS_2 (*a*) or pure CCl_4 (*c*); · · · · · · ·, 25 per cent CCl_4 (*a*,), (*b*), (*c*); – – – –, 50 per cent CCl_4 (*a*), (*b*), (*c*); – · – · – ·, 75 per cent CCl_4 (*a*), (*b*), (*c*). The arrows on the R axis indicate the limits of the first shell used to calculate the coordination numbers.

The first term in the expression represents the scattering due to the isolated molecules. It must be subtracted from the distinct part, in order to obtain the intermolecular part of the scattering containing information about correlations between atoms of different molecules. After this procedure, one calculates the Fourier transform of the distinct intermolecular scattering intensity

$$G_{\text{int}}(R) = 1 + \frac{2}{2\pi^2\rho R}\int_0^\infty \left[\left(\frac{d\sigma}{d\Omega}\right)_{\text{coh}}^{\text{dist, int}} \Big/ \bar{b}^2\right] \cdot \sin(\kappa R)\kappa d\kappa, \tag{7}$$

which can be written as a linear conbination of APCFs

$$G_{\text{int}}(R) = \sum_{i=1}^{N}\sum_{j=1}^{N} x_i x_j \sum_{\alpha=1}^{n_i}\sum_{\beta=1}^{n_j} \bar{b}_{i\alpha}\bar{b}_{j\beta}\, g_{i\alpha j\beta}(R), \tag{8a}$$

$$\bar{b} = \sum_{i=1}^{N} x_i \sum_{\alpha=1}^{n_i} b_{i\alpha}(\kappa), \qquad \bar{b}_{i\alpha} = b_{i\alpha}(\kappa)/\bar{b}. \tag{8b}$$

The intermolecular pair correlation function (IPCF) $G_{int}(R)$ is a weighted sum of all APCFs. In the case of the liquid mixture CCl_4/CS_2 it may be written

$$G_{int}(R) = a \cdot g_{C_BC_B}(R) + b \cdot g_{C_BS}(R) + c \cdot g_{SS}(R) + d \cdot g_{C_AC_A}(R) + e \cdot g_{ClC_A}(R) + f \cdot g_{ClCl}(R) + g \cdot g_{C_AC_B}(R) + h \cdot g_{C_AS}(R) + i \cdot g_{ClC_B}(R) + j \cdot g_{C_AS}(R). \quad (9)$$

C_A, C_B stand for the C-atom in CCl_4 and CS_2 respectively. To simplify the notation from now on we will drop the index 'int' so that $G(R)$ will refer to the IPCF.

In principle, it is possible to determine all APCFs by a set of an equal number of independent neutron scattering experiments by varying the scattering length of the scattering atoms by isotopic substitution whenever such isotopes are available.

4. Simulated correlation functions

4.1. *Centre–centre correlation functions*

All three centre–centre pair correlation functions (CCF) of the types '*BB*', '*AB*', and '*AA*' have been calculated for each composition of the mixture. These functions are plotted in figures 1 (*a–c*). The exact location of the extrema of these functions are presented in table 3. As we can see in figure 1 all CCFs exhibit two distinct peaks. In agreement with the size/shape of the two component molecules the peaks are at smaller distances for CS_2–CS_2, at significantly larger distances for CCl_4–CCl_4 and roughly at intermediate distances for the CS_2–CCl_4 peaks. In the case of the CS_2–CS_2 and CCl_4–CS_2 CCFs the first peak appears to be double, obviously reflecting the anisotropic shape of the CS_2 molecule. For a given pair the first peak changes only in amplitude when the concentrations are varied whereas the second peak displays a significant shift for all three CCFs. These changes gives us a hint as to the structural changes taking place when one component is gradually diluted with the other. It appears that the effect of introducing CS_2 molecules into the

Table 3. Positions and amplitudes of the extrema of the centre–centre radial correlation functions. The two species CCl_4 and CS_2 represented by '*A*' and '*B*' respectively.

	Conc. mol % CCl_4	I. Maximum		I. Minimum		II. Maximum	
		Posit. Å	Ampl.	Posit.	Ampl.	Posit.	Ampl.
AA	100	5·7	2·19	8·0	0·57	11·1	1·19
	75	5·6	2·11	7·0	0·61		
	50	5·7	2·09	7·7	0·61		
	25	5·7	1·97	7·7	0·66	9·6	1·06
AB	75	4·9–5·7	1·63	7·4	0·72		
	50	4·9–5·7	1·58	7·3	0·72		
	25	4·9–5·7	1·52	7·3	0·74	9·1	1·08
BB	75	4·1/5·0	1·27/1·51	7·2	0·77		
	50	4·1/5·0	1·23/1·49	7·0	0·77		
	25	4·1/5·0	1·17/1·45	6·9	0·83		
	100	4·1/5·0	1·08/1·41	6·9	0·85	8·6	1·06

immediate neighbourhood of CCl_4 changes the composition of the first shell but not the basic structure. The shifts of the second shell, on the other hand, indicate that at this distance from the central molecule we also have rearrangement of the structure. Thus, for example, figure 1 (*c*) shows that on introducing increasing amounts of CS_2 to CCl_4 the first shell is simply depleted of CCl_4 while an increasing amount of CCl_4 molecules appear in the region between the two shells probably as a consequence of the smaller volume occupied by the CS_2 molecules in the first shell and the different orientations the long axis of CS_2 can take on the surface of a CCl_4 molecule. We thus clearly observe a rearrangement of the CCl_4 structure, these molecules being expelled from the first shell and finding new sites between the first and the second shell. Figure 1 (*a*) shows a similar behaviour of the CS_2 molecules when CCl_4 is introduced. Figure 2 illustrates in a pictorial form the changes of the CCF of a mixture of the type studied. On the basis of these CCFs we have defined the first coordination shell of an '*A*' molecule as the region in which the '*A*' molecules can be in contact. The region beyond this limit is considered as the second coordination shell. A definition of the shell boundary based on the minimum of the CCFs is less useful since the minimum shifts with changes of the mole fraction. The adequacy of this definition of the coordination shells is additionally corroborated by the observation that the position and width of the first peak changes little with composition.

On the basis of the area under the first peak of the simulated CCFs we calculated the partial coordination numbers Z_A^A, Z_B^A, Z_A^B, Z_B^B. The upper index indicates whether the central molecule, i.e. the molecule around which the coordination

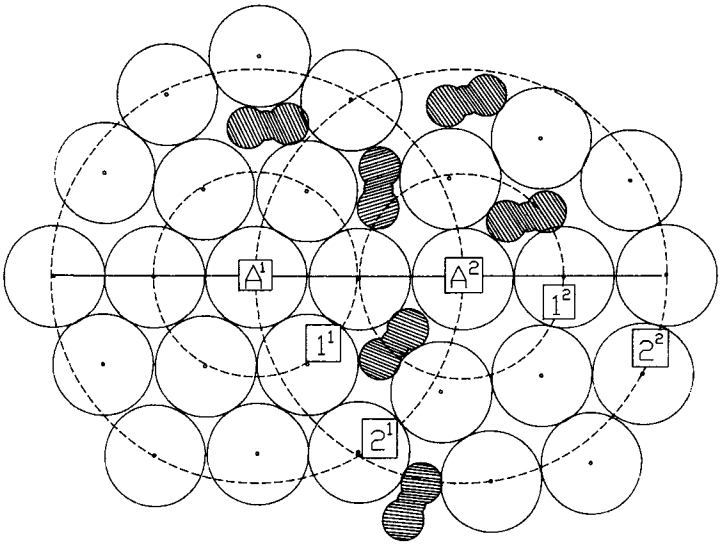

Figure 2. Local structure in the neighbourhood of type '*A*' molecules: The first and the second coordination shells of molecules A^1 and A^2 are indicated. The first coordination shell 1^1 remains undisturbed while the corresponding shell 1^2 is modified by introduction of type '*B*' molecules. The second coordination shells are both modified either directly by inclusion of type '*B*' molecules or indirectly as a consequence of the destruction of the ordered arrangement in the first shell. 1^2 also illustrates the shift of the peak maximum towards larger R_{CC}-values as type '*B*' molecules are introduced into the first shell. The different broadening of the first and the second coordination peaks in $g(R)$ as shown in figure 1 are also illustrated.

Table 4. The total and the partial coordination numbers from the first shell.

Conc. mol % CCl_4	00	25	50	75	100
Z_A^A		3·5	6·4	8·7	10·8
Z_B^A		9·7	5·9	2·6	
Z_A^B		3·2	5·9	7·9	
Z_B^B	14·0	8·8	5·2	2·3	
Z^A		13·2	12·3	11·3	10·8
Z^B	14·0	12·0	11·1	10·2	

number is an '*A*' or a '*B*' molecule

$$\xi_j^i := \frac{Z_j^i}{Z_A^i + Z_B^i}. \tag{10}$$

The indices i and j both run over A and B. The total coordination numbers in the first shell of '*A*' and '*B*' molecules respectively are represented by Z^A and Z^B.

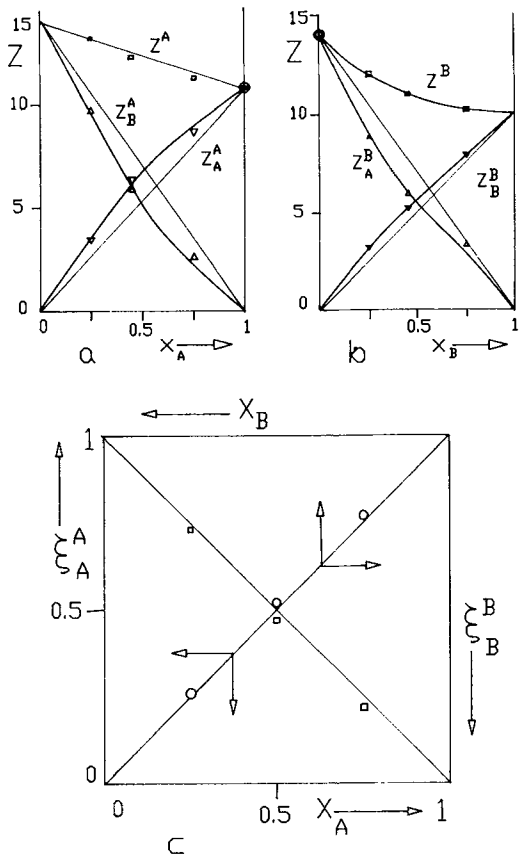

Figure 3. A plot of the coordination numbers in the first shell of an A (*a*) and a B (*b*) molecule. (*c*) shows the molecular fractions ξ_A^A and ξ_B^B vs. the bulk mole fractions.

Table 5. Local concentrations of the components $A \equiv CCl_4$ and $B \equiv CS_2$.

Conc. mol % CCl_4	ξ_A^A	ξ_B^A	ξ_A^B	ξ_B^B	ξ_S
100	1·0	—	—	—	—
75	0.77	0.23	0.77	0.23	1.0
50	0·52	0·48	0·53	0·47	0·99
25	0·26	0·74	0·27	0·73	0·99
0				1·0	1·0

$$Z^A = Z_A^A + Z_B^A, \tag{11a}$$

$$Z^B = Z_B^B + Z_A^B. \tag{11b}$$

The calculated coordination numbers are given in table 4. This is also illustrated in figures 3(*a*)–(*c*). Figures 3(*a*), (*b*) show the coordination numbers in the first shell of an A and a B molecule respectively. We see that the partial coordination numbers in the first shell in both cases do not vary linearly with the mole fractions. However, if we plot the molecular fractions ξ_A^A and ξ_B^A vs. the bulk mole fractions x_A and x_B,

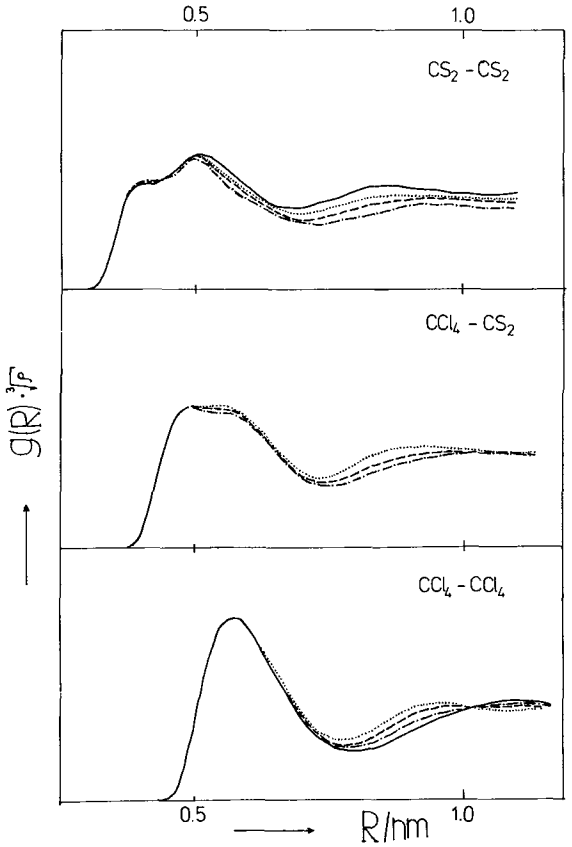

Figure 4. The CCFs as displayed in figure 1 scaled by the factor $3\sqrt{\rho}$.

respectively, we see that indeed the composition of the first shell is practically identical with the bulk composition. This shows that, in spite of the positive enthalpy of mixing reported for this system [6], no clustering effect is observed in the model mixture. The small deviations of the molecular fractions from the bulk mole fractions of the component A and B in figure 3 (*c*) is a result of the uncertainty in the choice of shell limits. The deviations from the ideal lines in figures 3 (*a*), (*b*) is due to the difference in surface requirement of the two molecules involved.

The molecular fractions as defined in equation (10) are listed in columns 2–5 of table 5. Column 6 contains the values of the quantity ξ_s defined as

$$\xi_s = \sum \xi_i^i, \tag{12}$$

The index i runs over all components. Deviations of ζ_S from the value 1·0 have been used to indicate the degree of cluster formation [13]. As can be seen from the table the values of ξ_s lie, for the model system studied, within computational error very near 1·0. This result clearly indicates that the average local molecular fraction is indeed equal to the bulk mole fraction.

In order to rationalize the variations of the amplitude of the CCFs with the mole fractions of the components one can attribute these effects to the difference in surface and volume requirements of molecules as different in shape and size as CCl_4 and CS_2. These considerations on the effects of dimensionality, i.e. volume vs. surface requirements in the first shell have led us to scale the CCFs in figure 3 at different concentrations with the factor $(\rho)^{1/3}$. Figure 4 illustrates the result and shows that in the low R range the scaling indeed brings the plots to coincidence.

4.2. *Atom pair correlation functions*

The functions $g_{\alpha\beta}(R)$ obtained from the simulation at the mole fraction of $x_A = 0{\cdot}5$ are illustrated in figure 5. The location of the extrema are listed in table 7. We should note that the APCFs do not change dramatically in the concentration range studied. In a forthcoming publication we shall report on the further analysis of these APCFs in view of obtaining a more detailed picture of the liquid mixtures. For the moment we shall restrict the application to the calculation of the simulated IPCFs $G^{MD}(R)$.

Table 6. The different sets of the coefficients *a–j* in arbitrary units (see equation (9)) from the neutron experiments as the isotopes: *a'*, ^{35}Cl; *b'*, ^{37}Cl; *c'*, ^{nat}Cl.

	a'	*b'*	*c'*
a	0·010	0·043	0·012
b	0·018	0·074	0·021
c	0·008	0·032	0·009
d	0·010	0·043	0·014
e	0·144	0·169	0·158
f	0·503	0·165	0·458
g	0·021	0·087	0·026
h	0·124	0·145	0·129
i	0·145	0·169	0·150
j	0·018	0·074	0·022

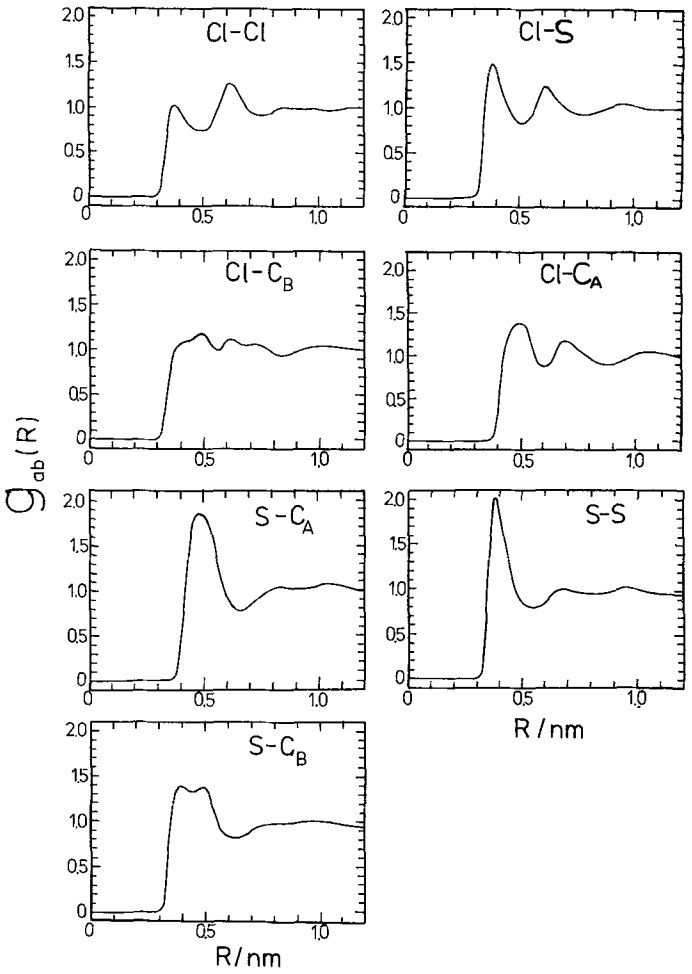

Figure 5. The atom–atom pair correlation functions APCFs obtained from this MD-simulation study at equimolar concentration.

Table 7. Positions and amplitudes of the extrema [Pos. (Å)/Ampl. (a.u.)] of the APCFs $g_{\alpha\beta}(R)$ at 50% mole fraction CS_2 in CCl_4.

$g_{\alpha\beta}(R)$	Maxima			Minima	
Cl–Cl	3·80/1·02	6·10/1·22	8·5/1·00	5·0/0·71	7·5/0·89
Cl–S	3·90/1·5	6·11/1·21	9·5/1·05	5·1/0·80	7·9/0·90
Cl–C_A	5·0/1·35	7·0/1·15	10·05/1·05	6·0/0·85	8·9/0·87
Cl–C_B	4·9/1·25	6·0/1·10	7·15/1·05	10·0/1·00	5·5/0·96 6·6/1·01 8·4/0·9
S–S	3·9/2·00	6·9/0·99	9·05/1·0	5·5/0·80	8·2/0·9
S–C_A	4·9/1·86	8·24/1·01	10·05/1·05	6·6/0·8	9·2/1·0
S–C_B	3·9/1·39	4·95/1·35	9·85/1·0	4·4/1·3	6·2/0·8

C_A = C atom of CCl_4, C_B = C atom of CS_2.

4.3. *Intermolecular pair correlation functions*

Experimental IPCFs $G^N(R)$ for the mixture CCl_4/CS_2 have been recently obtained by neutron scattering in a collaborative project [10]. In this study only three independent neutron diffraction experiments could be carried out on the isotopically substituted molecules $C^{35}Cl_4/CS_2$, $C^{37}Cl_4/CS_2$ and $C^{nat}Cl_4/CS_2$ at room temperature and equimolar compositions. The intermolecular contribution to the diffraction pattern has been Fourier transformed and an experimental IPFC $G^N(R)$ was constructed. The values of the coefficients *a–j* from equation (9) for each neutron experiment are shown in table 6. Although the experimental data do not suffice to determine the APCFs some interesting comparisons can be made between $G^N(R)$ and $G^{MD}(R)$ obtained from these data and from the present simulation.

Figures 6(*a'*)–(*c'*) illustrate these two IPCFs. The figures show a remarkably good agreement between the experimental and the simulated IPCFs. Thus, the steep initial increase, the location and the shape of the first peak and, finally, the second peak are in excellent agreement. The agreement also extends to some of the local structure in the region of the first peak. This result amply justifies the use of the described potential model and indicates that the structural data of the mixtures can be considered as quite reliable.

Using equation (9) with coefficients from table 6 and the values of the relevant APCFs one can easily estimate the percent contribution of each APCF to the total IPCF which are shown in table 8. From this table, one can conclude that the first

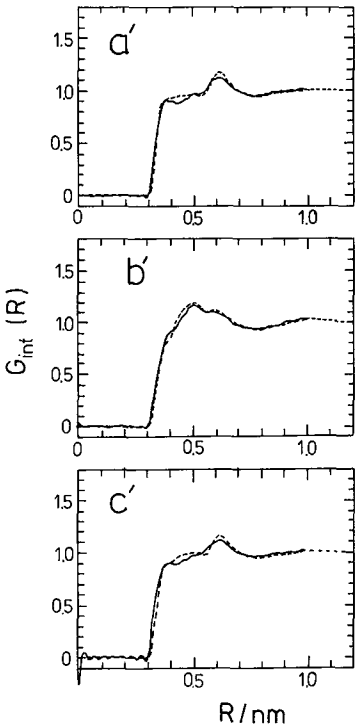

Figure 6. Comparison between experimental (———) and calculated (– – – –) intermolecular pair correlation functions (IPCFs) at equimolar concentration. *a'*, $C^{35}Cl_4/CS_2$; *b'*, $C^{37}Cl_4/CS_2$; *c'*, $C^{nat}Cl_4/CS_2$.

Table 8. The relative (per cent) contributions of the APCFs to the total $G_{int}(R)$ function at $R = 6{\cdot}1$ Å. The dash means a value approximately zero.

	Coef. · $g_{\alpha\beta}(R)$; $R = 6{\cdot}1$ Å									
$G_{int}(R)$	C–C_B	S–C_B	S–S	C_A–C_A	Cl–C_A	Cl–Cl	C_A–C_B	Cl–S	Cl–C_B	S–C_A
a'	1	1	—	2	11	53	3	13	14	2
c'	1	2	1	3	12	49	3	13	14	2
	Coef. · $g_{\alpha\beta}(R)$; $R = 5{\cdot}0$ Å									
b'	5	8	3	3	19	10	12	10	17	12

peak of $G(R)$ at $R = 6{\cdot}1$ Å has its main contribution from the second peak of $g_{Cl-Cl}(R)$. This actually contributes with more than 50 per cent. Other relevant contributions come from the APCFs $g_{Cl-C_B}(R)$, and $g_{Cl-S}(R)$ further contributions being rather small.

The situation is different in the case illustrated in figure 6(b') where the IPCF exhibits a peak at 5·0 Å with an amplitude 1·2 and a second peak located at the same position as in the other cases, with an amplitude 1·1. From the numbers given in table 9 we see that the main contribution of the APCFs to the first peak are the contributions from $g_{Cl-C_A}(R)$, $g_{Cl-C_B}(R)$, $g_{C_A-C_B}(R)$ and $g_{S-C_B}(R)$. It is also interesting to note that the correlations $g_{Cl-Cl}(R)$, $g_{Cl-S}(R)$ and $g_{S-C_B}(R)$ contribute by approximately 28 per cent. The other contributions are quite small but not negligible. In other words, the construction of the peak at 5·0 Å has a more cooperative character in terms of APCFs than the first peak in the other cases illustrated in figures 6(a'), (c'). It also appears that for the IPCF in figure 6(b') similar considerations apply to the peak at 6·1 Å, which is present in this function, too.

5. Summary and conclusions

In this paper MD-simulation results on three mole fractions of the liquid mixtures CCl_4/CS_2 at room temperature are reported. The main results obtained by this study can be summarized as follows:

(*a*) It has been shown that the proposed atom–atom potential model for the CCl_4/CS_2 liquid mixture is quite reliable. It enables a quantitative prediction of the intermolecular pair correlation functions obtained by neutron scattering.

(*b*) All centre–centre and atom–atom pair correlation functions have been calculated and discussed. The general conclusion which emerges from our results is that the change of composition results only in changes of the concentration and particle density in otherwise intact first coordination shell while it leads to serious structural changes in the second coordination shell. These effects have been interpreted in terms of molecular volume and shape differences between the two kinds of molecules involved. Finally, no formation of homomolecular clusters is observed in this system.

This study was carried out within the project 'Complex Liquids' of the 'Zentrum für interdisziplinäre Forschung' (ZiF) of the University of Bielefeld. Also, the financial support of the 'Fonds der Chemischen Industrie' is gratefully acknowledged.

References

[1] ANDERSON, H. C., WEEKS, J. D., and CHANDLER, D., 1971, *Phys. Rev.* A, **4,** 1597. WEEKS, J. D., CHANDLER, D., and ANDERSON, H. C., 1971, *J. chem. phys.*, **54,** 5237. FISCHER, J., and LADO, S., 1983, *J. chem. Phys.*, **78,** 5750.

[2] BOHN, M., FISCHER, J., and KOHLER, F., 1986, *Fluid Phase Equilib.*, **31,** 233.

[3] FINCHAM, D., QUIRKE, N., and TILDESLEY, D. J., 1986, *J. chem. Phys.*, **84,** 4535. EVANS, M. W., 1987, *J. chem. Phys.*, **86,** 4096. FINCHAM, D., QUIRKE, N., and TILDESLEY, D. J., 1987, *J. chem. Phys.*, **87,** 6117.

[4] STEINHAUSER, O., and NEUMANN, M., 1980, *Molec. Phys.*, **40,** 115. MCDONALD, I. R., BOUNDS, D. G., and KLEIN, M. L., 1982, *Molec. Phys.*, **45,** 521.

[5] STEINHAUSER, O., and NEUMANN, M., 1979, *Molec. Phys.*, **37,** 1921. TILDESLEY, D. J., and MADDEN, P. O., 1981, *Molec. Phys.*, **42,** 1137.

[6] HLAVATY, K., 1970, *Czech. Chem. Commun.*, **35,** 2878. HARSTED, B. S., and TMOMSEN, E. S., 1975, *J. chem. Thermodyn.*, **7,** 369. SIDDIQI, M. A., and LUCAS, K., 1981, *J. chem. Thermodyn.*, **15,** 1181.

[7] CZWORNIAK, K. J., ANDERSEN, H. C., and PECORA, R., 1975, *Chem. Phys., II,* 451. SIDDIQI, M. A., KRAHN, W., and LUCAS, K., 1987, *J. chem. engng Data*, **32,** 48.

[8] SHAPIRO, L., and BROIDA, H. P., 1967, *Phys. Rev.*, **154,** 129. HIGASHIGAKI, Y., WHITTENBURG, S. L., and WANG, C. H., 1978, *J. chem. Phys.*, **69,** 3297. VERSMOLD, H., 1978, *Ber. Bunsenges phys. Chem.*, **82,** 451. POTTHAST, L., SAMIOS, J., and DORFMÜLLER, Th., 1986, *Chem. Phys.*, **102,** 147.

[9] COON, J. E., GUPTA, S., MCLAUGHLIN, E., 1987, *Chem. Phys., II,* **3,** 43.

[10] GÜNSTER, S., ZEIDLER, M. D. (to be published).

[11] DORE, J. C., 1983, *Molecular Liquids—Dynamics and Interactions*, edited by A. J. Barnes, W. J. Orville-Thomas, and I. Yarwood (Proceedings of the NATO Advanced Study Institute on Molecular Liquids—Dynamics and Interactions, Florence), p. 411.

[12] BARTSCH, E., BERTAGNOLLI, H., and CHIEUX, P., 1986, *Ber. Bunsenges. phys. Chem.*, **90,** 34.

[13] SCHOEN, M., and HOHEISEL, C., 1984, *Molec. Phys.*, **53,** 1367.